

Raman Scattering Study of Phase Biaxiality in a Thermotropic Bent-Core Nematic Liquid Crystal

Min Sang Park,¹ Beom-Jin Yoon,¹ Jung Ok Park,^{1,2} Veena Prasad,⁴ Satyendra Kumar,⁵ and Mohan Srinivasarao^{1,2,3}

¹*School of Polymer, Textile and Fiber Engineering, Georgia Institute of Technology, Atlanta, Georgia, USA*

²*Center for Advanced Research on Optical Microscopy (CAROM), Georgia Institute of Technology, Atlanta, Georgia, USA*

³*School of Chemistry and Biochemistry, Georgia Institute of Technology, Atlanta, Georgia, USA*

⁴*Center for Liquid Crystal Research, Jalahalli, Bangalore 560013, India*

⁵*Department of Physics, Kent State University, Kent, Ohio, USA*

(Received 14 January 2009; published 8 July 2010)

Polarized Raman spectroscopy was used to investigate the development of orientational order and the degree of phase biaxiality in a bent-core mesogenic system. The values of the uniaxial order parameters $\langle P_{200} \rangle$ and $\langle P_{400} \rangle$, and biaxial order parameters $\langle P_{220} \rangle$, $\langle P_{420} \rangle$, and $\langle P_{440} \rangle$, and their evolution with temperature were determined. The temperature dependence of almost all order parameters reveals a second order transition from the uniaxial to biaxial nematic phase with $\langle P_{220} \rangle$ increasing to ~ 0.22 before a first order transition to the smectic-C phase, upon cooling.

DOI: 10.1103/PhysRevLett.105.027801

PACS numbers: 61.30.-v

The biaxial nematic, N_b , phase has been one of the most elusive liquid crystalline phases since its prediction by Freiser [1,2] in 1970 based on his generalization of the Maier-Saupe model [3] of the uniaxial nematic, N_u , phase. This prediction was followed by a number of important microscopic [4–6] and phenomenological [7–9] models, and by simulations [10] which yield interesting phase diagrams with one biaxial nematic, N_b , phase and two (prolate and oblate) uniaxial nematic, N_u , phases. In the microscopic models, the biaxiality was either due to molecular shape biaxiality [4,5] or a consequence of mixing rodlike and platelike objects [6]. Quite remarkably, they all lead to phase diagrams with similar topology having two N_u phases, one (N_u^+) with positive $S [= 0 \rightarrow +1]$ and the other (N_u^-) having negative $S [= 0 \rightarrow -1/2]$. The transitions between the isotropic (I) and the N_u^-/N_u^+ (or, N_u^\pm) phases are predicted to be first order while the transitions from the N_u^\pm to the N_b phase form lines of second order transitions.

Encouraged by the success of the work of Saupe and co-workers in discovering the N_b phase in a lyotropic liquid crystalline system [11], several attempts were made to verify its existence in thermotropic systems [12–14] which were proved unsuccessful [15]. However, recent discoveries of the N_b phase using x-ray diffraction [16] and NMR [17] have rekindled the scientific interest in nematic biaxiality. These discoveries have inspired theorists [18,19] as well as experimentalists [20–23] to inquire into the physics of this hitherto elusive but scientifically interesting phase.

At the transition to the N_b phase, the growth of (biaxial) orientational order (OO) in a direction perpendicular to \mathbf{n} is described by a two-component order parameter. Here \mathbf{n} , known as the nematic director, describes the average direction of alignment of the molecular axes. This transition thus falls in the two-dimensional-XY universality class [24]. An essential step toward understanding their rich phenomenology is to quantify the degrees of OO and its

evolution as a function of temperature, through the various phase transitions.

In this Letter, we report the results of our Raman scattering study of the evolution of orientational order in a bent-core compound A131 [25], which possesses both the N_u and N_b phases, thereby permitting measurements of thermal evolution of distinct orientation modes associated with the uniaxial and biaxial OO parameters. The valuable information presented here will help explain phase transitions and dynamics of thermotropic biaxial nematic liquid crystals.

Unlike the orientation of the conventional N_u phase with perfect symmetry cancellation, in the N_b phase, there is breaking of the continuous rotational symmetry about the nematic director, \mathbf{n} . Thus, a more elaborate form of the orientation distribution function (ODF) must be used to express the degree of orientation in the N_b phase. A set of orthogonal functions of Euler angle (α, β, γ) can be used to construct a simple ODF expansion. This will enable us to transform the orientation dependence of physical quantities in the macroscopic (or laboratory) frame XYZ to their orientation dependence in the molecular frame xyz . The ODF is generally expressed as [26]

$$f(\alpha, \beta, \gamma) = \sum_{L=0}^{\infty} \sum_{m,n=-L}^L \frac{2L+1}{8\pi^2} \langle D_{mn}^{L*} \rangle D_{mn}^L(\alpha, \beta, \gamma), \quad (1)$$

where $D_{mn}^L(\alpha, \beta, \gamma)$ are the Wigner rotation matrices and $\langle D_{mn}^L \rangle$ indicates the statistical average of $D_{mn}^L(\alpha, \beta, \gamma)$. Depending on the values of $L (L \in \mathbb{N})$, the ODF is made up of a set of $(2L+1)^2$ Wigner matrices [26]. However, if there are certain symmetries in both sample and molecular systems, a number of components are left out of consideration, so that ODF can be simplified [27]. Figure 1 depicts the experimental geometry where the orientation of a particular unit with respect to a coordinate system may be described by the Euler angles, α, β, γ . For simplicity, it is usually assumed that the Raman probe is axially sym-

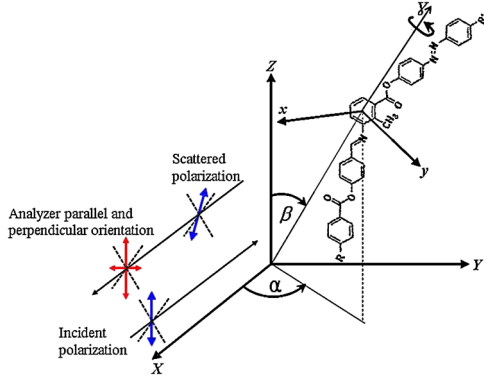


FIG. 1 (color online). Euler angles α , β , γ are defined with molecular axes xyz in a macroscopic (laboratory) system of axes XYZ . The polarization of the Raman scattered light is resolved by the different direction of the analyzer.

metric. Thus, one may assume a random rotation about the

$$f(\alpha, \beta) = \frac{1}{8\pi^2} \left\{ \begin{aligned} &1 + \frac{5}{2}\langle P_{200} \rangle(3\cos^2\beta - 1) + 15\langle P_{220} \rangle(1 - \cos^2\beta)\cos(2\alpha) \\ &+ \frac{9}{8}\langle P_{400} \rangle(3 - 30\cos^2\beta + 30\cos^4\beta) \\ &+ \frac{135}{2}\langle P_{420} \rangle(-1 + 8\cos^2\beta - 7\cos^4\beta)\cos(2\alpha) \\ &+ \frac{315}{4}\langle P_{440} \rangle(1 - 2\cos^2\beta + \cos^4\beta)\cos(4\alpha) \end{aligned} \right\}. \quad (2)$$

Based on the geometry in Fig. 1, the intensity of polarized Raman scattering is a function of the electric field and the ODF integrated over all possible orientations, and can be expressed as

$$I_{ij}(\theta) = k\alpha_{ij}^2 \int_{\alpha} \int_{\beta} f(a, \beta) (E_{ij}(\alpha, \beta, \theta))^2 \sin\beta d\alpha d\beta, \quad (3)$$

where k is a proportionality constant that depends on factors such as incident light intensity, instrumental transmission, light collection efficiency, etc., θ is the angle between the incident polarization direction and the symmetry axis of the Raman probe, and $E_{ij}(\alpha, \beta, \theta)$ is the electric field vector with rotational degrees of freedom about α , β , θ . This enables us to obtain coefficients of ODF from the measurements of I_{ij} . The notation I_{ij} denotes the scattering intensity analyzed in the i direction (in

Euler angle γ and, as a result, the order parameters $\langle D_{mn}^L \rangle$ only have values other than zero when $n = 0$. In addition, mirror symmetry of a sample fixes m to be even. Hence, we can expand this matrix in terms of the series of Legendre polynomials, $\langle P_{Lm0} \rangle$. Since the study of polarized Raman spectroscopy allows us to obtain quantitative information about molecular orientation up to fourth orientation order parameters, ODF in this study can be expanded in terms of 5 coefficients, $\langle P_{200} \rangle$, $\langle P_{400} \rangle$, $\langle P_{220} \rangle$, $\langle P_{420} \rangle$, and $\langle P_{440} \rangle$. Note that the two parameters, $\langle P_{200} \rangle$ and $\langle P_{400} \rangle$, commonly recognized as the uniaxial OO parameters, inform about the average orientation of molecules distributed along the z direction with dependence only on the angle β . In contrast, $\langle P_{220} \rangle$, $\langle P_{420} \rangle$, and $\langle P_{440} \rangle$ characterize symmetry with a possible average over only the γ angle; thus nonzero values of these biaxial OO parameters are indicative of the existence of biaxial symmetry. To simplify, the ODF can be expressed [26] by $f(\alpha, \beta)$ as

our geometry, $i \equiv Z, Y$) with incident polarization in the j direction (in our geometry, $j \equiv Z, Y$). Expanding Eq. (3) with our suitable geometry gives the reduced expression of Raman intensities, $I_{\parallel} = I_{ZZ}(\theta)$ and $I_{\perp} = I_{YZ}(\theta)$, accomplished by resolving polarized light intensity into the parallel and perpendicular direction of the analyzer. Furthermore, a series of spectra were recorded over the entire range of 0 to 2π at 10° interval by rotating the samples relative to the fixed direction of polarization of the incident light. It is because a range of orientations of the polarizer and analyzer with respect to the symmetry axes of the LC provides more detailed information than only parallel and perpendicular polarizations of laser excitation [28,29]. Consequently, we can derive expressions for the depolarization ratio, $R(\theta) = I_{\perp}/I_{\parallel}$, which is of importance in determining the Raman tensor, and write

$$R(\theta) = \frac{(-1+r)^2 \left\{ \begin{aligned} &-40\langle P_{200} \rangle - 240\langle P_{220} \rangle + (105\cos 4\theta - 9)\langle P_{400} \rangle \\ &-(228 + 1260\cos 4\theta)\langle P_{420} \rangle + 210\sin^2 2\theta\langle P_{440} \rangle \end{aligned} \right\}}{\left\{ \begin{aligned} &40(4r^2 - r - 3)[\langle P_{200} \rangle(1 + 3\cos 2\theta) + 12\langle P_{220} \rangle\sin^2 \theta] \\ &-3(r-1)^2\langle P_{400} \rangle(9 + 20\cos 2\theta + 35\cos 4\theta) \\ &-1200(r-1)^2\langle P_{420} \rangle\sin^2 \theta(3 + 7\cos 2\theta) \\ &-5607\sin^2 \theta\langle P_{440} \rangle - 8(56r^2 + 28r + 21) \end{aligned} \right\}}, \quad (4)$$

where $r = \alpha'_{yy}/\alpha'_{zz}$ is the Raman tensor ratio.

In this study, 15 μm thick LC cells with homogeneous director alignment were used. Homogeneous (uniaxial nematic) director alignment was ascertained under crossed polarizers using a polarizing optical microscope. The polarized Raman spectra were obtained using a $10\times$ dry

objective and a 785 nm laser light source (Kaiser Optic Systems). We used a compound A131, for which the most intense peak is the one at 1141 cm^{-1} attributed to the asymmetric stretching of C-O-C [30]. It is noteworthy that strong Raman effects correspond to internal vibrations of the mesogenic units, whose dipole moments are likely to

be oriented along their long molecular axes (in the z direction in Fig. 1). It allows us to assume collinearity of the principal axes of the Raman tensor with the molecular axes. Figure 2(a) is an example of the experimental data for $I_{ZZ}(\theta)$, $I_{YZ}(\theta)$, and $R(\theta)$ of A131. $I_{ZZ}(\theta)$ and $I_{YZ}(\theta)$ are normalized to unity at the peak of I_{ZZ} . The pattern of twofold and fourfold rotational symmetry of $I_{ZZ}(\theta)$ and $I_{YZ}(\theta)$ is conformable to trigonometric periodicities of expansion in Eq. (2) for $I_{ZZ}(\theta)$ and $I_{YZ}(\theta)$, respectively [28].

These polarized Raman spectra over a wide range of incident angles were fit to Eq. (4) using the polynomial fit function in MATHEMATICA. This resulted in six fitting parameters, namely, uniaxial order parameters, $\langle P_{200} \rangle$ and $\langle P_{400} \rangle$, biaxial order parameters, $\langle P_{220} \rangle$, $\langle P_{420} \rangle$, and $\langle P_{440} \rangle$, and r . It is necessary to note that there may be as many as 6 coefficients from Eq. (4) for a fit, if the evaluation is done without some constraints. Using Eq. (4), the calculated depolarization ratio, $R(\theta)$, is shown in Fig. 2(b), with the theoretical fit.

We determined temperature dependence of $\langle P_{200} \rangle$, $\langle P_{400} \rangle$, $\langle P_{220} \rangle$, $\langle P_{420} \rangle$, and $\langle P_{440} \rangle$ by making measurements

of $I_{ZZ}(\theta)$ and $I_{YZ}(\theta)$ and calculating $R(\theta)$ through the various phases which A131 exhibits, i.e., I - N_u , N_u - N_b , and N_b -smectic- C transitions upon cooling. We assumed that the biaxial terms are negligible in the estimation of the uniaxial order parameters and Raman tensor ratio, $r = \alpha'_{yy}/\alpha'_{zz}$. Based on these approximations, biaxial order terms play a significant role for the fits. Figure 3 is a plot of various order parameters as a function of temperature, $T - T_{NI}$ ($^{\circ}\text{C}$). Among the biaxial OO parameters, the high value of $\langle P_{220} \rangle$ provides quantitative evidence that one of the molecular short axes is preferentially aligned perpendicular to the ZY plane. The fourth rank order parameters, $\langle P_{420} \rangle$ and $\langle P_{440} \rangle$, have a more complicated physical interpretation. The observed negative values, in particular, for $\langle P_{440} \rangle$, indicate that the direction of the chain axis is projected onto the XY plane at approximately $\pm 45^{\circ}$ to the X or Y axis, rather than collinear to them, since the value of $(1 - 2\cos^2\beta + \cos^4\beta)$ is positive for all β . The absolute limits for the 3 biaxial order parameters, $\langle P_{220} \rangle$, $\langle P_{420} \rangle$, and $\langle P_{440} \rangle$, can be easily calculated, as was done by Jarvis *et al.*, [31] and can be written as

$$\left| \langle P_{220} \rangle = \frac{1}{4} \langle (1 - \cos^2\beta) \cos 2\alpha \rangle \right| \leq \frac{1}{4} = 0.25, \quad \left| \langle P_{420} \rangle = \frac{1}{24} \langle (-1 + 8\cos^2\beta - 7\cos^4\beta) \cos 2\alpha \rangle \right| \leq \frac{3}{56} = 0.0536, \\ \left| \langle P_{440} \rangle = \frac{1}{16} \langle (1 - 2\cos^2\beta + \cos^4\beta) \cos 4\alpha \rangle \right| \leq \frac{1}{16} = 0.0625. \quad (5)$$

It is worth noting that a previous report quantifying biaxial order parameters was not in agreement with the limit of analytical values of Eq. (5) [32]. By contrast, our results for the biaxial terms, displayed in Fig. 3, lie well within the absolute limits of the values throughout the temperature range studied.

To determine the changes in the order parameters at the phase transition from the $N_u \rightarrow N_b$ phase, we performed analysis at small temperature intervals. From the inset of Fig. 3, it is clear that an abrupt change in order parameter does not occur at the ($N_u \rightarrow N_b$) transition temperature, ruling out a first order transition. However, there is a qualitative change in the temperature dependence of these parameters at the transition. It is clearly seen in the case of uniaxial order parameters in Fig. 4. $\langle P_{200} \rangle$ and $\langle P_{400} \rangle$ increase in the uniaxial phase with decreasing temperature and level off, while in the biaxial phase both the parameters

increase until the discontinuous transition to the smectic- C phase occurs. Judging from the changes in the slope of these parameters, we conclude that the $N_u \rightarrow N_b$ phase transition is of second order. Based on the discontinuous nature of the variation of $\langle P_{200} \rangle$ and $\langle P_{400} \rangle$, we conclude $N_b \rightarrow$ smectic C to be of first order.

An interesting observation is that the value of $\langle P_{200} \rangle$ (~ 0.275) at $T - T_{NI} = -0.1^{\circ}\text{C}$ is smaller than the expected value of 0.35–0.4 for conventional uniaxial nematics. Theoretically, it is predicted that the biaxial order parameter fluctuations may drive the I - N_u transition to be second order [33]. It is likely that the biaxial order parameter fluctuations in the uniaxial nematic phase are responsible for this behavior. Hence, we compared the thermal fluctuations of A131 with those of $E7$ close to T_{NI} and observed much more pronounced fluctuations in the case of A131. A detailed analysis of the fluctuation at or close to

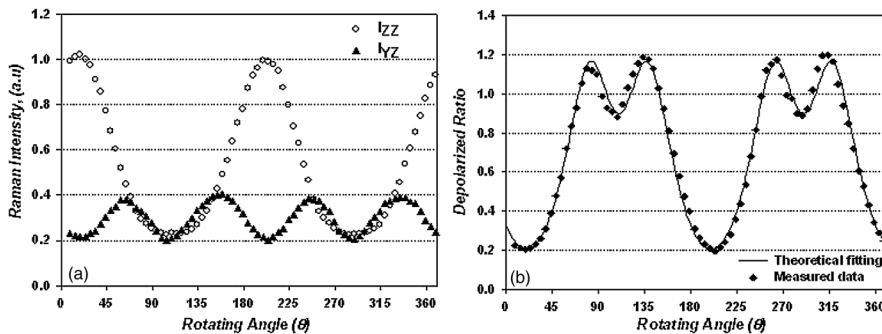


FIG. 2. (a) The Raman scattered light intensity profiles for A131 at 166.5°C and (b) the corresponding depolarization ratio profile; measured (\blacklozenge) and theoretical fit (solid line), using $\langle P_{200} \rangle = 0.381$, $\langle P_{400} \rangle = 0.207$, and $r = -0.1983$.

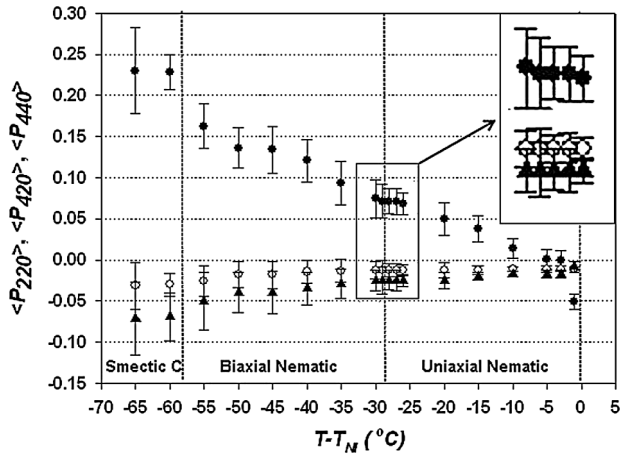


FIG. 3. Temperature dependence of biaxial order parameters: $\langle P_{220} \rangle$ (●), $\langle P_{420} \rangle$ (○), and $\langle P_{440} \rangle$ (▲), obtained by fitting the depolarization ratio profile, $R(\theta)$.

the phase transition will be published elsewhere [34]. This is consistent with the results of the study of the order parameter and director fluctuations by Sprunt *et al.* [35].

In summary, the quantitative and qualitative analyses of OO in the nematic phase strongly support the existence of the biaxial nematic phase in A131 from ~ 30 to 58°C below T_{NI} . We have demonstrated the power of the polarized Raman scattering technique in reliably measuring nematic order parameters and revealing their thermal evolution across the second order uniaxial to biaxial nematic phase transition, and at the first order biaxial nematic to smectic-C phase transition. The technique and the results presented here have a significant impact on our ability to quantitatively understand OO in nematic fluids and test theoretical prediction of shear flow aligning behavior and calculations of viscosities and elastic constants [36,37], the thermodynamic properties, and the rheological behavior of anisotropic fluids.

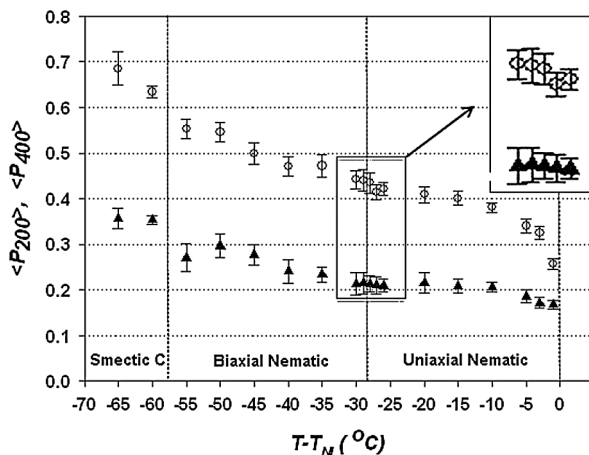


FIG. 4. Temperature dependence of uniaxial order parameters: $\langle P_{200} \rangle$ (○) and $\langle P_{400} \rangle$ (▲), obtained by fitting the depolarization ratio profile, $R(\theta)$.

This work was supported, in part, by the Office of Basic Energy Sciences, Department of Energy, Grant No. DE-SC0001412.

- [1] M. J. Freiser, *Phys. Rev. Lett.* **24**, 1041 (1970).
- [2] M. J. Freiser, *Mol. Cryst. Liq. Cryst.* **14**, 165 (1971).
- [3] W. Maier and A. Saupe, *Z. Naturforsch.* **13A**, 564 (1958).
- [4] R. Alben, *Phys. Rev. Lett.* **30**, 778 (1973).
- [5] J. P. Straley, *Phys. Rev. A* **10**, 1881 (1974).
- [6] R. Alben, *J. Chem. Phys.* **59**, 4299 (1973).
- [7] D. W. Allender, M. A. Lee, and N. Hafiz, *Mol. Cryst. Liq. Cryst.* **124**, 45 (1985).
- [8] M. C. J. M. Vissenberg, S. Stallinga, and G. Vertogen, *Phys. Rev. E* **55**, 4367 (1997).
- [9] P. Toledano, O. G. Martins, and A. M. Figueiredo Neto, *Phys. Rev. E* **62**, 5143 (2000).
- [10] D. Frenkel and R. Eppenga, *Phys. Rev. Lett.* **49**, 1089 (1982).
- [11] L. J. Yu and A. Saupe, *Phys. Rev. Lett.* **45**, 1000 (1980).
- [12] S. Chandrasekhar *et al.*, *Pramana* **30**, L491 (1988).
- [13] J. F. Li *et al.*, *Europhys. Lett.* **25**, 199 (1994).
- [14] L. Longa, J. Stelzer, and D. Dunmur, *J. Chem. Phys.* **109**, 1555 (1998).
- [15] G. R. Luckhurst, *Thin Solid Films* **393**, 40 (2001).
- [16] B. R. Acharya, A. Primak, and S. Kumar, *Phys. Rev. Lett.* **92**, 145506 (2004).
- [17] L. A. Madsen *et al.*, *Phys. Rev. Lett.* **92**, 145505 (2004).
- [18] L. Longa and G. Pajak, *Liq. Cryst.* **32**, 1409 (2005).
- [19] D. Allender and L. Longa, *Phys. Rev. E* **78**, 011704 (2008).
- [20] J. L. Figueirinhas *et al.*, *Phys. Rev. Lett.* **94**, 107802 (2005).
- [21] R. Y. Dong *et al.*, *Chem. Phys. Lett.* **448**, 54 (2007).
- [22] K. Merkel *et al.*, *Phys. Rev. Lett.* **93**, 237801 (2004).
- [23] K. Neupane *et al.*, *Phys. Rev. Lett.* **97**, 207802 (2006).
- [24] A. M. Sonnet, E. G. Virga, and G. E. Durand, *Phys. Rev. E* **67**, 061701 (2003).
- [25] V. Prasad *et al.*, *J. Am. Chem. Soc.* **127**, 17224 (2005).
- [26] C. Zannoni, *The Molecular Dynamics of Liquid Crystals* (Kluwer Academic Publishers, Dordrecht, The Netherlands, 1994), p. 11.
- [27] M. Vangurp, *Colloid Polym. Sci.* **273**, 607 (1995).
- [28] W. J. Jones *et al.*, *J. Mol. Struct.* **708**, 145 (2004).
- [29] C. D. Southern and H. F. Gleeson, *Eur. Phys. J. E* **24**, 119 (2007).
- [30] L-V. Daimay, *The Handbook of Infrared and Raman Characteristic Frequencies of Organic Molecules* (Academic Press, Boston, 1991), p. 61.
- [31] D. A. Jarvis *et al.*, *Polymer* **21**, 41 (1980).
- [32] C. D. Southern *et al.*, *Europhys. Lett.* **82**, 56001 (2008).
- [33] P. G. de Gennes and J. Prost, *The Physics of Liquid Crystals* (Clarendon Press, Oxford, 1993), p. 85.
- [34] B-J Yoon, M. S. Park, J. O. Park, and M. Srinivasarao (to be published).
- [35] J. A. Olivares *et al.*, *Phys. Rev. E* **68**, 041704 (2003).
- [36] L. A. Archer and R. G. Larson, *J. Chem. Phys.* **103**, 3108 (1995); R. G. Larson and L. A. Archer, *Liq. Cryst.* **19**, 883 (1995).
- [37] M. Fialkowski, *Phys. Rev. E* **55**, 2902 (1997); **58**, 1955 (1998).